

# From Calorimetry to Equations of State

Stanislaw L. Randzio

Polish Academy of Sciences, Institute of Physical Chemistry, ul. Kasprzaka 44/52, 01-224 Warszawa, Poland

## 1 Introduction

Equations of state (EOS) used in the description of the properties of matter are very interesting, effective, and intellectually stimulating because they facilitate an easy exploration of modern computational techniques, and further allow a deeper examination of many physicochemical questions, such as structure formation occurring in liquid or amorphous phases. EOS are also extremely important in solving practical problems concerning the exploitation of geothermal energy, oil and gas recovery, high-pressure organic synthesis, etc. Although a large number of semi-empirical and theoretical EOS (often developed with the use of statistical thermodynamic theories) have considerably advanced the general knowledge in the field, there are unfortunately many difficulties in the correct use of EOS over large ranges of pressure and temperature. Pressure (density) effects are in particular very difficult to handle by means of the known EOS. One of the reasons for this is the lack of a reference state at high densities which could be used as a high density verification of EOS and their construction. The absence of such a state can be compensated by selection of a distinctive thermodynamic property which should be measurable over large ranges of pressure and temperature by a convenient experimental technique. The present review is intended to demonstrate that the isobaric coefficient of thermal expansion,  $a_p(T,p) = 1/V_m(\partial V_m/\partial T)_p$  (where  $V_m$  is the molar volume), can be used as such a property, and that pressure-controlled scanning calorimetry can serve as a technique for its measurement.

## 2 Outline

The possibility of controlling the three most important thermodynamic variables ( $p, V, T$ ) in scanning calorimetric measurements makes it possible to realize simultaneous measurements of changes (or rates of such changes) of both thermal and mechanical contributions to the thermodynamic potential caused by the perturbation of one of the independent variables while the other independent variables are kept constant.<sup>1</sup> For example, the simultaneous recording of both the heat flow and the volume changes resulting from a given isothermal pressure scan leads to

Stanislaw Randzio is a research group leader in the Institute of Physical Chemistry of the Polish Academy of Sciences, Warsaw. He has a M.Sc. degree from the Department of Chemistry of Warsaw University, and Ph.D. and Habilitation degrees from the Institute of Physical Chemistry of the Polish Academy of Sciences. He has carried out post-doctoral work at the Thermochemical Centre at Lund and has been visiting professor at Brigham Young University, Blaise-Pascal University at Clermont-Ferrand, and at the Universities of Bochum and Cologne. He is an associate member of the IUPAC Commission on Chemical Thermodynamics.



the simultaneous determination of both  $(\partial S/\partial p)_T$  and  $(\partial V/\partial p)_T$ . The pressure derivatives of thermodynamic functions are particularly interesting because they provide important information about the intermolecular interactions in condensed matter, as has been demonstrated in the case of dense liquids.<sup>2,3</sup> The pressure variable has often been neglected in the thermodynamic investigation of liquids, although even at the beginning of this century Bridgman pointed out its role in testing the theories of liquids.<sup>4</sup> The present article is mainly concerned with the role of pressure as an independent variable in thermodynamic investigations.<sup>5</sup> The precision of calorimetric measurements of pressure derivatives performed over large ranges of pressure and temperature is 1–3%, depending on the pressure and temperature, and is much higher than the precision of the best volumetric techniques. Careful studies of a series of liquids of various physicochemical nature have revealed some characteristic features, such as the crossing of isotherms of the isobaric coefficient of thermal expansion ( $a_p$ ), minima in the isobaric heat capacity ( $C_p$ ) isotherms, a unique crossing point of  $a_p$  isotherms for simple liquids, the shifting of the crossing point to higher pressures with addition of an associative component, etc.

Some of the problems outlined above, such as the crossing point of  $a_p$  isotherms can be approached from the point of view of the hole theory and the concepts of metastable liquids which are based on the use in the correlation equation of the spinodal line as the stability limit for the liquid state.<sup>6–12</sup> This is an elegant way of correlating experimental data and to create empirical equations of state, but unfortunately this approach does not significantly advance our molecular knowledge of the dense liquid state. The intermolecular interactions in dense liquids have long been of interest to many scientists. The best known van der Waals EOS is based on the attractive potential determined by London dispersion forces and the hard sphere repulsive potential.<sup>13</sup> As pointed out by Leland and Chapman,<sup>14</sup> van der Waals himself (and also Boltzmann) recognized that the hard sphere term  $RT/(V_m - b)$  does not correctly account for the effect of molecular repulsion at high densities. Despite many later improvements of the van der Waals equation (e.g. references 15–17, and for recent remarks see reference 18) until very recently no previous EOS could reproduce the high-pressure experimental observations outlined above. By deriving a set of  $a_p$  isotherms from various EOS which were selected on the basis of their construction with respect to the repulsive and attractive contributions to the internal energy, and comparing the derived quantities with the experimental calorimetric observations, it was determined that the softness of the repulsive potential is the most important feature of the EOS under investigation towards the correct description of the high-density properties of liquids.<sup>19</sup> The use of the Maxwell distribution method<sup>20</sup> has allowed arrival at a repulsive term based on the Lennard-Jones potential, the shape of which can be varied by selecting various values for the exponents  $m$  and  $n$ .<sup>21</sup> A detailed analysis has revealed that the best reproduction (very close to the experimental observations) of the thermal expansivities for dense simple liquids, including the crossing point of isotherms, is obtained when the shape of the repulsive branch of the intermolecular potential is of the form of the 8–4 Lennard-Jones potential.<sup>19,21</sup>

The present review will start with a short presentation of a pressure-controlled scanning calorimeter as applied for determination of  $a_p$  for both liquid and solid substances. Then a comparison will be presented between sets of experimental

isotherms and isotherms derived from various EOS of  $a_p$  for *n*-hexane and methane, both treated as simple liquids. A similar comparison will also be presented for *n*-hexanol and its binary mixtures with *n*-hexane, treated as associated liquids. Also, a calorimetric verification of a theoretical EOS for polyethylene, both for crystalline and amorphous phases at pressures up to 300 MPa, will be presented. The author hopes that the present article will show that pressure-scanning calorimetry is a very good guide in searching for better EOS which should be useful not only in describing the properties of substances over wide ranges of pressure and temperature, but also towards a better understanding of the behaviour of dense matter.

### 3 Pressure-controlled Scanning Calorimetry

A presentation of the thermodynamic basis for scanning calorimetry controlled by an independent thermodynamic variable was given elsewhere,<sup>22</sup> thus only a brief introduction to a procedure in which pressure is taken as the inducing variable will be given here. The most important problem concerns the transmission of pressure into the investigated substance which is placed in the calorimetric vessel. The direct placement of a piston directly in the calorimetric vessel would lead to an enormous heat effect caused by friction, and thus a neutral hydraulic fluid is usually taken as an intermediate medium transmitted through a capillary, and the piston is then placed outside of the calorimeter. This experimental arrangement is presented in Figure 1a, where the sample under investigation is in mechanical contact with the hydraulic fluid within the calorimetric vessel. If there is a risk of chemical interaction between the hydraulic fluid and the substance under investigation, then the sample is placed in an ampoule, a bellows, *etc.* It should be noticed that in such an arrangement a part of the inner active volume  $V_m$  of the calorimetric vessel is filled by the hydraulic fluid and eventually by the ampoule. The active volume  $V_m$  is that part of the high-pressure tubing which exchanges heat directly with the calorimetric detector. This experimental design is most often used for investigations of solid substances. Figure 1b shows the experimental set-up used when the investigated sample is in the fluid state, and the whole internal volume  $V_m$  is filled with the substance under investigation through which the pressure variations are transmitted into the calorimetric vessel. In this case the number of moles  $N$  of the substance under investigation contained in the active volume  $V_m$  is changing during the pressure variations and is equal to  $V_m/V_m$ , where the molar volume of the substance,  $V_m$ , is a function of pressure. The transport of the hydraulic fluid (Figure 1a) and/or of the substance under investigation (Figure 1b) in/out of the calorimetric vessel during the pressure variations is always performed under isothermal conditions. This can be satisfactorily achieved if the heat exchangers are properly constructed and the heat effect is measured by means of a heat-flow or power compensated calorimeter.<sup>22</sup>

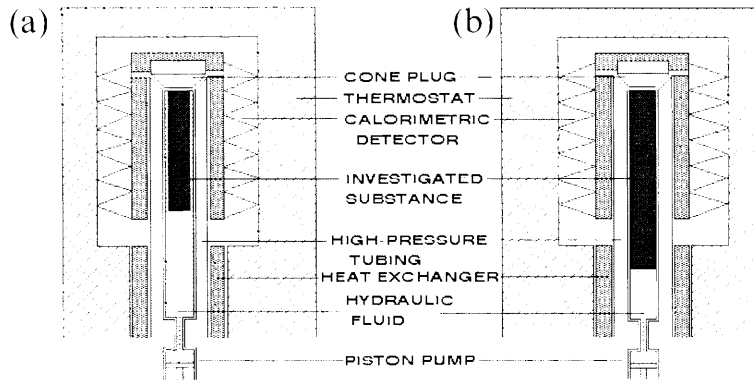


Figure 1 A schematic presentation of the calorimetric vessel arrangements for two methods of transmitting pressure into the substance under investigation during pressure-scanning measurements.

### 3.1 Determination of $a_p$ for Fluids

The enthalpy differential for one mole of a pure substance is described by the following equations:

$$dH_m(T,p) = \left( \frac{\partial H_m}{\partial T} \right)_p dT + \left( \frac{\partial H_m}{\partial p} \right)_T dp \quad (1)$$

$$dH_m(T,p) = dQ_m + V_m dp \quad (2)$$

When the temperature is kept constant and the pressure is varied as a linear function of time ( $T = \text{const.}$ ,  $dT = 0$ ,  $p = p_0 \pm at$ ,  $dp = \pm adt$ ), then  $N$  moles of the substance contained in the sample under investigation and submitted to such thermodynamic conditions will exchange heat at a rate defined by

$$\begin{aligned} \frac{dQ}{dt} &= P_T(p) = \pm N \left[ \left( \frac{\partial H_m}{\partial p} \right)_T - V_m \right] a \\ &= \pm N \left( \frac{\partial S_m}{\partial p} \right)_T Ta = -N \left[ \pm \left( \frac{\partial V_m}{\partial T} \right)_p Ta \right] \end{aligned} \quad (3)$$

where  $P_T(p)$  is the power generated or absorbed under isothermal conditions. For the experimental arrangement presented in Figure 1b  $N = V_{in}/V_m$ , equation 3, can thus be reduced to the following form:

$$P_T(p) = - \left[ \pm \frac{1}{V_m} \left( \frac{\partial V_m}{\partial T} \right) V_{in} Ta \right] = -(\pm a_p V_{in} Ta) \quad (4)$$

where  $a_p$  is the isobaric coefficient of thermal expansion of the substance under investigation. The power generated or absorbed by such process in the cylindrical wall of the calorimetric vessel can be described by the following equation:<sup>23</sup>

$$P_{T,w}(p) = \pm a_{p,w} V_{in} Ta \quad (5)$$

where  $a_{p,w}$  is the isobaric coefficient of thermal expansion of the material from which the calorimetric vessel is made. From equations 4 and 5 the final expression for the calorimetric determination of  $a_p$  for fluids is:

$$a_p = - \frac{\Delta P_T(p)}{V_{in} Ta} + a_{p,w} \quad (6)$$

where  $\Delta P_T(p)$  is the total power recorded in the stationary state by the calorimetric detector as a response to the inducing pressure variations occurring at rate  $a$ . The internal volume  $V_{in}$  is determined in calibration measurements by filling the calorimetric vessel with a fluid of known  $a_p(p, T)$ . The pressure can also be scanned as a series of stepwise changes  $\Delta p_n$ , where the calorimetric output signal is then recorded as a series of thermograms.<sup>24</sup> In this case equation 6 takes the following form:

$$\langle a_{p,n} \rangle = -\frac{Q_n}{V_{in} T \Delta p_n} + a_{p,w} \quad (7)$$

where  $\langle a_{p,n} \rangle$  is the mean value of the isobaric thermal expansion coefficient over the applied pressure step, and  $Q_n$  is the quantity of heat obtained from integration of the respective calorimetric thermogram. An expression similar to equation 7 was used by Ter Minassian and Pruzan<sup>25</sup> in their piezothermal technique where the pressure variations were realized as a series of manual quasi-stepwise changes. Figure 2a and b show results from the determination of  $a_p$  as a function of pressure at 354.6 K for *n*-hexane and benzene, respectively, with the use of all the methods presented above and performed with various instruments. In the above graphic presentations the thermal expansivities obtained from respective reference tables prepared on the basis of the best volumetric measurements are also given (for references see Figure 2a and b). The agreement is satisfactory between both the calorimetric measurements and the reference tables. Unfortunately, the reference tables are limited in pressure, with tabulations only up to 100 MPa. At higher pressures the discrepancies of thermal expansivities obtained from volumetric measurements are much higher, up to 20–35 per cent.<sup>28</sup> Thus, the calorimetric methods for the determination of the thermal expansivities of liquids at high pressures are for the moment the most accurate.

### 3.2 Determination of $a_p$ for Solids

In the case of the experimental arrangement presented in Figure 1a, in addition to the thermal effects defined by equation 3 for the investigated sample and by equation 5 for the high-pressure tubing, there will be a thermal effect developed in the hydraulic fluid which fills up a part of the active volume equal to ( $V_{in} - NV_m$ ):

$$P_{T,f} = -[\pm aT(V_{in} - NV_m)a_{p,f}] \quad (8)$$

where  $a_{p,f}$  is the thermal expansivity of the hydraulic fluid. From equations 3, 5, and 8 the final expression for the calorimetric determination of  $a_p$  for solid materials is:

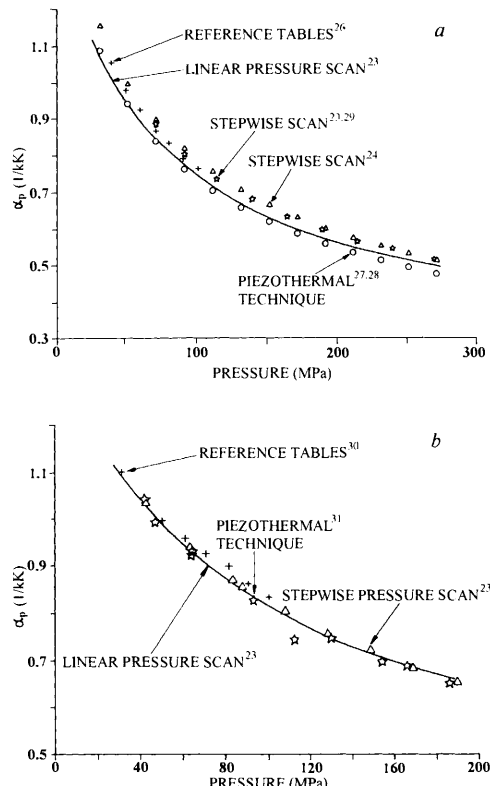


Figure 2 A comparison of results of  $a_p$  measurements as a function of pressure at 354.6 K. Various methods for *n*-hexane (a) and benzene (b).

It is worth noting that in the case when the whole internal volume of the calorimetric vessel is filled with the substance under investigation during the scanning of pressure, equation 9 is reduced to the simple form of equation 6 or 7. In all other cases the determination of  $a_p$  for solid materials requires knowledge of the thermal expansivity of the hydraulic fluid and of the volume of the material under investigation. When pressure scanning is carried out with a piston pump (Figure 1) driven by a stepping motor,<sup>1,5,23,24</sup> then by counting the number of motor steps  $N_s$  the volume variations of the sample under investigation caused by the pressure change can be determined by:

$$N \frac{dV_m}{dp} = k_s \left( \frac{dN_s}{dp} \right)_{tot} - k_s \left( \frac{dN_s}{dp} \right)_f \quad (10)$$

where  $k_s \approx 5 \times 10^{-6} \text{ cm}^3 \text{ step}^{-1}$  is the calibration constant of the piston-stepping motor system. The second term of equation 10 is concerned with the compressibility of the hydraulic fluid and is determined in calibration experiments when the whole volume is filled only with the hydraulic fluid. The first term is obtained during pressure-scanning calorimetric measurements by simultaneous recording of the number of motor steps as a function of pressure. For such case the volume of the material under investigation as a function of pressure at a given temperature  $T$  is determined by equation 11:

$$V_m(T, p) = V_m(T, p_0) - \int_{p_0}^p \frac{dV_m}{dp} dp \quad (11)$$

where  $V_m(T, p_0)$  is the molar volume of the substance under investigation at normal pressure, which can be determined by a simple pycnometer.

### 4 $a_p(p, T)$ for Simple Liquids: Experimental and Derived from Various EOS

Already in 1913 Bridgeman<sup>4</sup> reported from his volumetric measurements that at high pressures the  $a_p$  isotherms of liquids may cross and recross in a most bewildering way. As emphasized by Street<sup>32</sup> at least part of this unusual behaviour could be a result of errors in the measured volumes. Taking *n*-hexane as a test substance we have performed systematic measurements of  $a_p$  with pressure-controlled scanning calorimeters constructed in three different laboratories.<sup>1,23,24</sup> The results of these measurements, together with the data of other authors<sup>27,28</sup> obtained using the piezothermal technique,<sup>25</sup> were fitted by least-squares to a correlation equation.<sup>29</sup> The final result, which is presented in Figure 3a, clearly demonstrates that the  $a_p$  isotherms of *n*-hexane, taken over the temperature interval of 200 K, have a unique crossing point (■), occurring at  $70 \pm 3$  MPa, where  $a_p = (8.70 \pm 0.10) \times 10^{-4} \text{ K}^{-1}$ , and is independent of temperature. At lower pressures  $a_p$  increases with increasing temperature but at higher pressures, up to 700 MPa,  $a_p$  decreases with temperature increases. Such a characteristic experimental feature can be used as a diagnostic for EOS of dense simple liquids.<sup>19</sup> Most of the known EOS can be written in a form in which the repulsive and attractive contributions to the pressure can be separated. Below, results showing the derivation of that property from two groups of EOS (those with the attractive contribution modified with respect to the van der Waals EOS and those with a modified repulsive contribution) will be presented.

#### 4.1 $a_p$ Derived from EOS with a Modified Attractive Contribution

The isobaric thermal expansivities of *n*-hexane derived from the van der Waals EOS<sup>13</sup> and from selected EOS<sup>33–35</sup> (see Table 1)

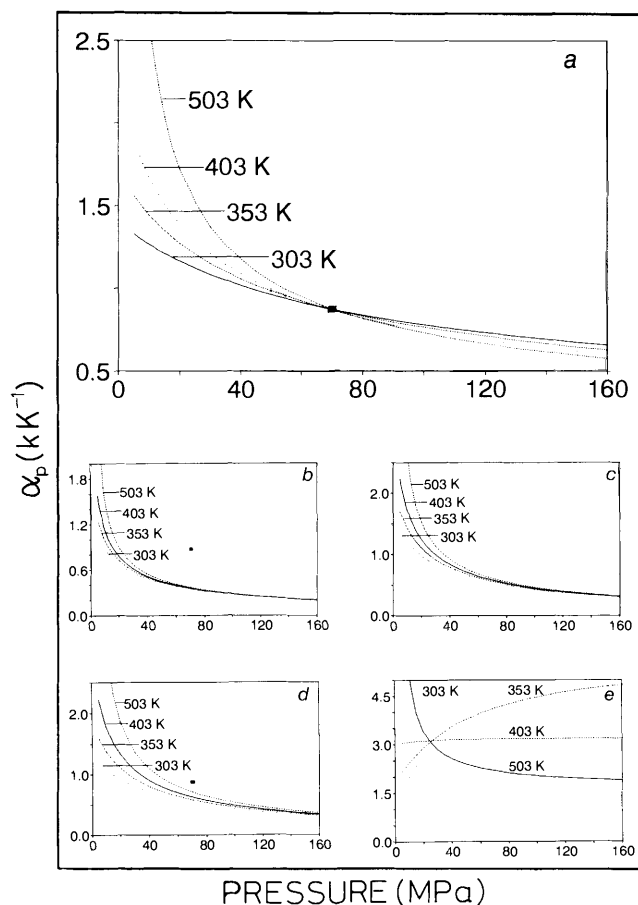


**Figure 3** Isobaric thermal expansivities  $\alpha_p$  for *n*-hexane: experimental (a)<sup>29</sup> and derived from the van der Waals EOS<sup>13</sup> (b, equation 12) and from EOS with a modified attractive contribution to the pressure: Redlich-Kwong<sup>33</sup> (c, equation 13), Soave<sup>34</sup> (d, equation 14), Peng-Robinson<sup>35</sup> (e, equation 15); ■, crossing point of isotherms derived from experimental data.

**Table 1** Selected equations of state of the van der Waals type with a modified attractive contribution to the pressure

NAME	EQUATION
van der Waals <sup>13</sup>	$p = \frac{RT}{V_m - b} - \frac{a}{V_m^2} \quad (12)$
	where $R$ is the ideal gas constant, $b$ is the co-volume and the parameter $a$ is proportional to the average intermolecular attractive force: the two parameters can be determined from the critical pressure $p_c$ and critical temperature $T_c$ :
	$b = RT_c/8p_c, a = 27R^2 T_c^2/64p_c$
Redlich-Kwong <sup>33</sup>	$p = \frac{RT}{V_m - b} - \frac{a}{V_m(V_m + b)\sqrt{T}} \quad (13)$
Soave <sup>34</sup>	$p = \frac{RT}{V_m - b} - \frac{a f(T_c, w)}{V_m(V_m + b)} \quad (14)$
	where $w$ is the acentric factor (for <i>n</i> -hexane $w = 0.296$ and for methane $w = 0.008$ )
Peng-Robinson <sup>35</sup>	$p = \frac{RT}{V_m - b} - \frac{a f(T_c, w)}{V_m(V_m + b) + b(V_m - b)} \quad (15)$

are presented in Figures 3b–e. The results demonstrate that the crossing point, or even any crossing of isotherms, cannot be obtained for *n*-hexane using the van der Waals<sup>13</sup> equation, or with similar equations with the modified attractive term, such as Redlich-Kwong<sup>33</sup> and Soave<sup>34</sup> EOS. An advanced complication of the temperature dependence of the attractive contribution in the Peng-Robinson<sup>35</sup> EOS results in the appearance of the crossing point, but at low temperatures (up to almost 403 K) the isotherms have incorrect character, with  $a_p$  increasing with increasing pressure, a trend opposite to that observed experimentally. Similar results have been also obtained for methane. A set of three isotherms for liquid methane derived from the IUPAC tables for that substance<sup>36</sup> are presented in Figure 4a. There is a similar crossing point (■), although it appears at higher pressure with respect to *n*-hexane. The isotherms of  $a_p$  for methane cross at  $p = 90 \pm 5$  MPa, where  $a_p = (1.893 \pm 0.019) \times 10^{-3} \text{ K}^{-1}$ .<sup>19</sup> Neither the van der Waals EOS nor the set of EOS with the modified attractive contribution presented in Table 1 correctly reproduce the experimental data for methane. One can speculate that a further complication of the attractive contribution could result in a proper representation of derived data both for methane and *n*-hexane, but most probably the physical significance of such a modification would be easily lost.

#### 4.2 $a_p$ Derived from EOS with a Modified Repulsive Contribution

In all EOS using the modified attractive contribution (Table 1 and Figures 1b–e) the repulsive contribution based on the

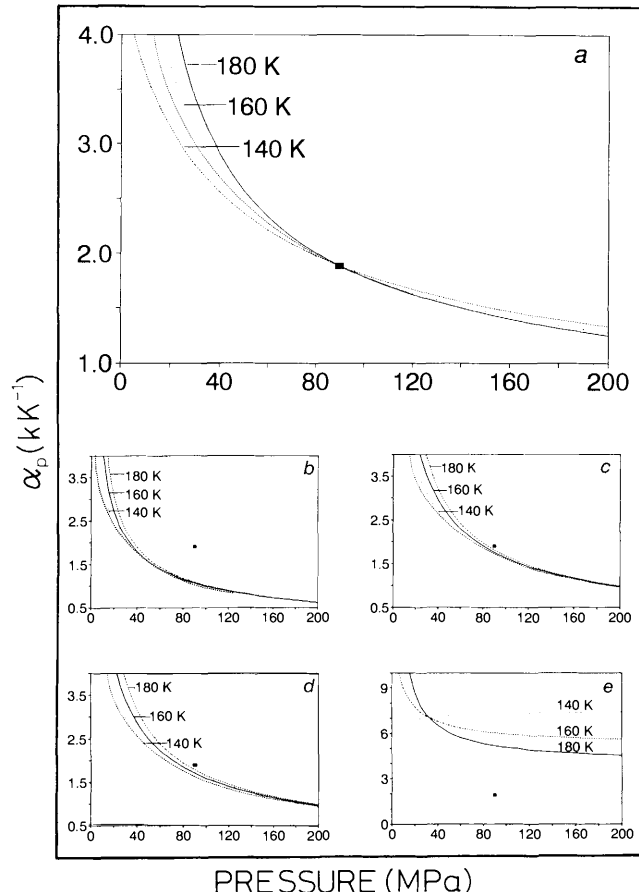


**Figure 4** Isobaric thermal expansivities  $\alpha_p$  for methane: experimental (a)<sup>19,36</sup> and derived from the van der Waals EOS<sup>13</sup> (b, equation 12) and from EOS with a modified attractive contribution to the pressure: Redlich-Kwong<sup>33</sup> (c, equation 13), Soave<sup>34</sup> (d, equation 14), Peng-Robinson<sup>35</sup> (e, equation 15); ■, crossing point of isotherms derived from experimental data.

simple rigid-sphere term  $RT/(V_m - b)$  remained unchanged. When the rigid-sphere term in the van der Waals EOS is replaced by the hard-sphere equation of Carnahan and Starling<sup>37</sup> [Table 2, equation 16, where  $\xi = (\pi\sqrt{2/6})(b/V_m)$ ], the behaviour of the derived  $a_p$  isotherms for both *n*-hexane (Figure 5a) and methane (Figure 5b) is correct over the entire ranges of pressure and temperature under investigation, although the crossing points of the isotherms in both cases are rather far from the experimental results. When the van der Waals attractive term is replaced by the temperature-dependent attractive contribution of Redlich and Kwong<sup>33</sup> (equation 17, Table 2) the derived thermal expansivities for both *n*-hexane (Figure 5c) and methane (Figure 5d) did not improve. In fact they are even worse with respect to the simple van der Waals attractive term. This observation is in opposition to the original suggestion of Carnahan and Starling that a modification of the attractive term can improve the behaviour of their equation at high densities.<sup>38</sup> The encouraging results obtained with the testing of Carnahan–Starling EOS at high densities are most probably related to the softness of the interaction potential, real molecules must have a softly repulsive potential. A step further in the understanding of this problem follows the soft-sphere repulsive term of Deiters and Randzio<sup>21</sup> based on the Lennard–Jones intermolecular potential and constructed with use of the Maxwell distribution method<sup>20</sup> (Table 2, equations 18–25, where  $\zeta_0 = (\pi/6) \cdot N\sigma^3/V_m$  and  $T = k_B T/\epsilon$ ;  $\sigma$  and  $\epsilon$  are size and energy parameters of a Lennard–Jones-type potential). Values of parameters  $a_1 \dots a_6$  can be calculated from equations 20–25 for various interaction potential shapes with the exponents of the repulsive part and of the attractive part ranging between ( $8 \leq m \leq 40$ ) and ( $4 \leq n \leq 8$ ), respectively. For

**Table 2** Selected equations of state of the van der Waals type with a modified repulsive contribution to the pressure

NAME	EQUATION
Carnahan–Starling <sup>37</sup> –van der Waals	$p = \frac{RT}{V_m} \left( 1 + \frac{4\xi - 2\xi^2}{(1 - \xi)^3} \right) - \frac{a}{V_m^2} \quad (16)$
Carnahan–Starling–Redlich–Kwong <sup>33</sup>	$p = \frac{RT}{V_m} \left( 1 + \frac{4\xi - 2\xi^2}{(1 - \xi)^3} \right) - \frac{a}{V_m(V_m + b)\sqrt{T}} \quad (17)$
	$p = \frac{RT}{V_m} \left( 1 + \frac{4\xi + a_5\xi^2 + a_6\xi^3}{(1 - \xi)^3} \right) - \frac{a}{V_m^2} \quad (18)$
	$\xi = \xi_0 \frac{a_1}{(1 + a_2 T^{1/n})^{1/m}} \quad (19)$
	$a_1 = \left( \frac{m}{n} \right)^{1/n} \quad (20)$
	$a_2 = \frac{1}{3} + \frac{6.75}{n} - \frac{13}{n^2} + \frac{m}{14 + 5n} - \frac{3.5}{m + n} \quad (21)$
Deiters–Randzio <sup>21</sup>	$a_3 = \frac{3}{5} \quad (22)$
	$a_4 = \frac{\frac{13}{9}}{\frac{5}{3} - \frac{4}{n} - \frac{m}{4}} \quad (23)$
	$a_5 = -2 \left( 1 + \frac{1}{m} + \frac{6}{mn} \right) \quad (24)$
	$a_6 = -\frac{4}{4 - \frac{6}{n} + \frac{m}{9}} \quad (25)$

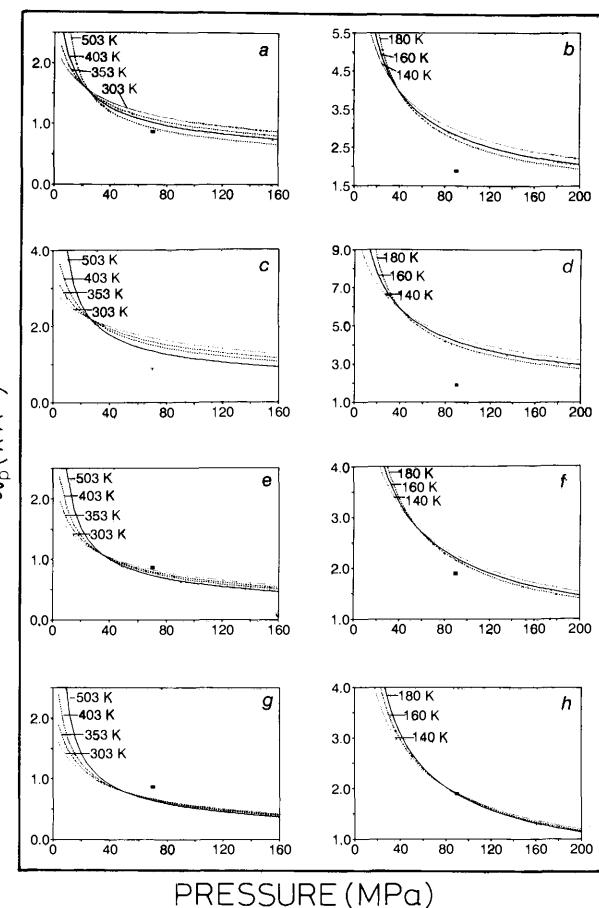


**Figure 5** Isobaric thermal expansivities  $a_p$  calculated from selected EOS of the van der Waals type with a modified repulsive contribution to the pressure for *n*-hexane and methane respectively: (a, b) Carnahan–Starling<sup>37</sup>–van der Waals<sup>13</sup> (equation 16); (c, d) Carnahan–Starling<sup>37</sup>–Redlich–Kwong<sup>33</sup> (equation 17); (e, f) Deiters–Randzio<sup>21</sup> (equations 18–25) for 12–6 interacting pair potential; (g, h) Deiters–Randzio<sup>21</sup> (equations 18–25) for 8–4 interacting pair potential: ■, crossing point of isotherms derived from experimental data.

the construction of the soft-sphere repulsive term only the repulsive branch of the potential is taken into consideration. The attractive contribution in the whole EOS is defined by the van der Waals attractive term (see equation 18). Examples of results obtained with this equation for the 12–6 Lennard–Jones potential are presented in Figure 5c for *n*-hexane and in Figure 5f for methane. The obtained results are much better than with the Carnahan–Starling EOS, although the crossing points of isotherms both for *n*-hexane and methane still appear at unexpectedly low pressures. The best results are obtained with the repulsive term constructed on the 8–4 Lennard–Jones potential. In the case of methane (Figure 5h) the agreement between derived values and the experimental data is almost perfect. In the case of *n*-hexane (Figure 5g) the agreement is less than perfect, most probably because *n*-hexane is much less spherical than methane.

### 5 $a_p(p, T)$ for Associated Liquids

The behaviour of  $a_p(p, T)$  for associated liquids is much more complicated than that for the simple liquids, and depends on the mechanism of the specific interactions. For example for *m*-cresol,<sup>39</sup> a self-associated liquid, there is no crossing point over the temperature range from 303 K to 503 K at pressures up to 400 MPa. The isotherms do cross near 100 MPa, but the crossing points are temperature dependent. The isotherms cross at lower pressures as temperature increases. A unique crossing point may exist at some high temperature where *m*-cresol is unassociated

since the low-temperature behaviour probably results from the association equilibrium. For water,<sup>40</sup> another self-associated liquid, the behaviour of  $\alpha_p(p, T)$  is even more complicated. At temperatures up to almost 323 K the isobaric thermal expansivities increase with increase in pressure, but all isotherms over the temperature range from 223 K (super-cooled water) up to 423 K cross near 400 MPa. Although the calorimetric technique has been very important in the establishment of the correct set of  $\alpha_p(p, T)$  data for water and *m*-cresol, the detailed analysis of the behaviour of such complicated liquids is out of the scope of the present review. However, additional attention will be given below to *n*-hexanol, also a self-associated liquid, and its binary mixtures with *n*-hexane.

Calorimetric measurements have demonstrated that with addition of *n*-hexanol to *n*-hexane the crossing of isotherms is pushed to higher pressures, almost as a linear function of *n*-hexanol concentration.<sup>41</sup> For illustration, Figures 6a and 6b show results of calorimetric measurements for 0.1 and 0.5 molar ratio mixtures of *n*-hexanol with *n*-hexane, respectively, whereas Figure 7c shows pure *n*-hexanol. None of the known EOS can reproduce the observed behaviour of  $\alpha_p(p, T)$ . Reasonable results have been obtained only with the Deiters equation which takes into account the volume change during association, and thus accounts for the pressure effects on the association equilibrium with the use of the so-called chain association theory.<sup>42</sup> However, the best results have so far been obtained by combining the soft sphere EOS<sup>21</sup> (based on the 8–4 Lennard–Jones potential and the van der Waals attractive term) and the chain-association

term from the Deiters equation.<sup>42</sup> A detailed presentation of this new equation will be given elsewhere. Figures 7a,b, and c show results of derivation of  $\alpha_p(p, T)$  for *n*-hexanol and its mixtures with *n*-hexane at the same concentrations as in Figure 6 which shows the results of calorimetric measurements. One can see that despite differences in the absolute values of thermal expansivities, the qualitative agreement is satisfactory. The existence of isotherm crossing and its shifting with pressure is almost the same as in the calorimetric measurements. Thus, by adding an association term<sup>42</sup> to the soft-sphere EOS<sup>21</sup> we could reproduce the shifting of the isotherm crossing to higher pressures with use of the critical data only of both substances, and the association properties in the ideal state. Further improvements of the equation are needed, and most probably such modifications should be related to the symmetry of the two molecules. The calorimetric information nevertheless represents an important test and provides certain guidelines for such studies.

## 6 $\alpha_p(p, T)$ for Crystal and Amorphous Phases of Polyethylene

The crystalline polyethylenes are examples of the coexistence of crystal and amorphous phases. The Pastine theoretical EOS for polyethylene<sup>43,44</sup> is composed of a crystal part constructed on the basis of precise crystallographic structural data, and an amorphous part constructed with the use of averaged structural assumptions. In a recent study<sup>45</sup> we have performed a series of  $\alpha_p$

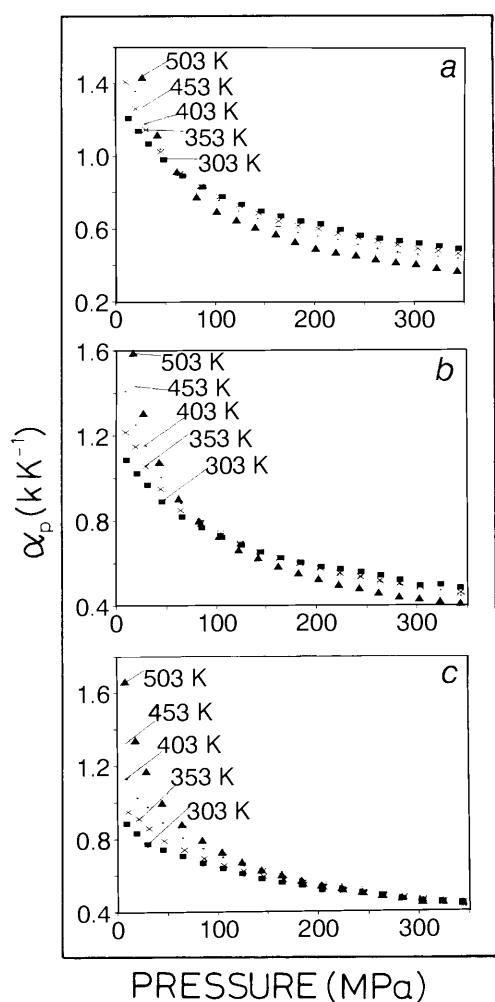


Figure 6 Direct calorimetric experimental data<sup>41</sup> on the isobaric thermal expansivities  $\alpha_p$  of *n*-hexanol (c) and its binary mixture with *n*-hexane: 0.1 molar ratio of *n*-hexanol (a) and 0.5 molar ratio of *n*-hexanol (b).

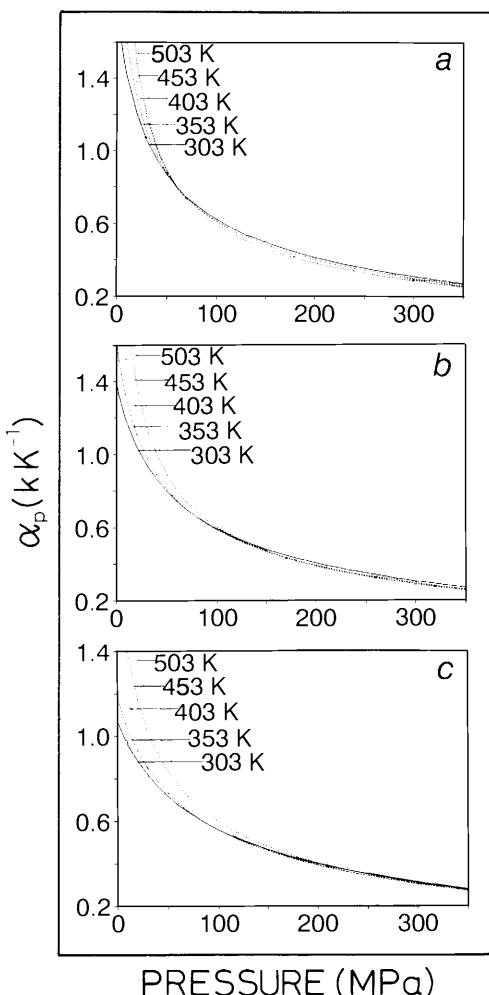


Figure 7 Isobaric thermal expansivities  $\alpha_p$  derived from a soft-sphere EOS<sup>21</sup> combined with a contribution for the chain-association accounting for the volume changes<sup>42</sup> for *n*-hexanol (c) and its binary mixture with *n*-hexane: 0.1 molar ratio of *n*-hexanol (a) and 0.5 molar ratio of *n*-hexanol (b).

measurements for polyethylenes of various crystallinities at several temperatures as a function of pressure up to 300 MPa. As an example, in Figure 8a three  $\alpha_p$  isotherms for low-density polyethylene (crystallinity  $\chi_c = 0.4$ ) are presented. One can see that the isotherms have a tendency to converge at high pressures, but they do not cross as was observed for simple liquids. This observation is limited to the pressure range under investigation. The measurements performed for polyethylenes of various crystallinities have shown that  $\alpha_p$  is a linear function of crystallinity over the whole  $(p, T)$  surface under investigation. From this observation  $\alpha_p$  for both crystal and amorphous phases could be determined by extrapolation to  $\chi_c = 1.0$  and  $\chi_c = 0.0$ . It is worth noting that the isotherms for the amorphous phase cross (see Figure 8b), and thus in this respect the behaviour of the amorphous phase is similar to the behaviour of a simple liquid. For the crystal phase (Figure 8c) the isotherms are almost parallel over the pressure range under investigation. The same  $\alpha_p$  isotherms for both the crystal and amorphous phases could also be derived from the Pastine theoretical EOS.<sup>44</sup> A comparison of  $\alpha_p$  derived from the Pastine EOS and  $\alpha_p$  extrapolated from the experimental data is presented in Figures 8a and 8b for the amorphous and crystal phases, respectively. One can see that for the crystal phase (Figure 8c) the agreement at atmospheric pressure is reasonable (at 333 K the agreement is almost perfect), but discrepancies appear with increase in pressure. For the

amorphous phase (Figure 8b) the agreement is less satisfactory both at low and high pressures. Most probably this can be explained by the approximative character of the amorphous part in the Pastine EOS.<sup>43</sup>

## 7 Other Thermodynamic Criteria

Brown<sup>46</sup> and later Rowlinson<sup>47</sup> have proposed thermodynamic criteria for EOS which should be satisfied, including the existence of the *Amagat line* where  $(\hat{C}U, \hat{C}V)_T = 0$ , or the *Charles line* where  $(\hat{C}H, \hat{C}p)_T = 0$ . Furthermore, second derivatives define two additional lines:  $(\hat{C}C_p, \hat{C}V) = 0$  and  $(\hat{C}C_p, \hat{C}p)_T = 0$ , where the isotherms of principal heat capacities show maxima or minima.<sup>47</sup> A disadvantage of these criteria is that they constitute qualitative tests only, because there are not enough experimental data on those derivatives over sufficiently large ranges of pressure and temperature. Practically all existing data, especially in the high pressure region, have been derived from empirical equations of state, often constructed in a predictive way, and thus cannot be used as reliable reference data. However, it is useful to recall that the minima at the isotherms of the isobaric heat capacity are practically determined by the behaviour of  $\alpha_p$  (equation 26):

$$\left( \frac{\hat{C}C_{p,m}}{\hat{C}p} \right)_r = - V_m T \left[ a^2 + \left( \frac{\hat{C}a_p}{\hat{C}T} \right)_r \right] \quad (26)$$

When the  $\alpha_p$  isotherms cross, a negative value of  $(\hat{C}a_p, \hat{C}T)_p$  appears which may cause  $(\hat{C}C_p, \hat{C}p)_T$  to become zero since  $a_p^2$  is always positive. Direct measurements of heat capacities at high pressures are very difficult, and there is no such high-pressure calorimeter working over a large range of temperature yet reported in the literature. Thus, the calorimetric data on  $\alpha_p(p, T)$  are presently also the most important experimental information on the pressure dependence of the heat capacity over large ranges of pressure and temperature. The exact values of  $C_p$  can thence be obtained through the equation of state. However, for that purpose the heat capacities at atmospheric pressure (or saturated vapour pressure) must also be accurately known as a function of temperature. This information can be obtained by temperature-controlled scanning calorimetry (DSC). As an example, Figure 9 shows isotherms of  $C_p$  for methane at 140 K derived using various EOS which are compared to the data obtained from reference tables.<sup>36</sup> Once again, one observes that the best reproduction of the experimental data is obtained with the soft-sphere EOS for which the repulsive contribution is based on the 8-4 Lennard-Jones potential.

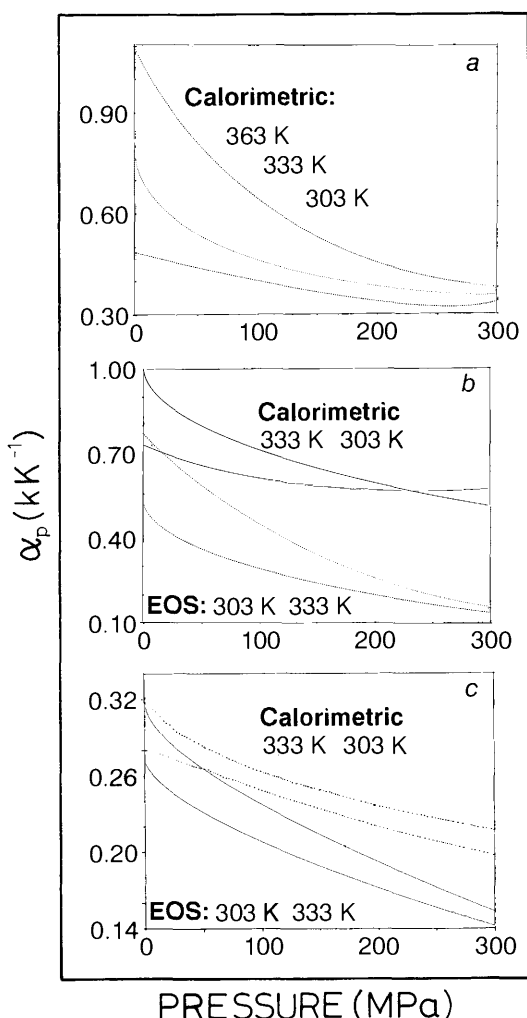


**Figure 8** Isobaric thermal expansivities  $\alpha_p$  for a crystalline polyethylene:<sup>45</sup> (a) experimental for low-density polyethylene (crystallinity  $\chi_c = 0.4$ ); (b) experimental (extrapolated) and calculated  $\alpha_p$  from the Pastine EOS<sup>43,44</sup> for the amorphous phase; (c) experimental (extrapolated) and calculated  $\alpha_p$  from the Pastine EOS<sup>43,44</sup> for the crystal phase.

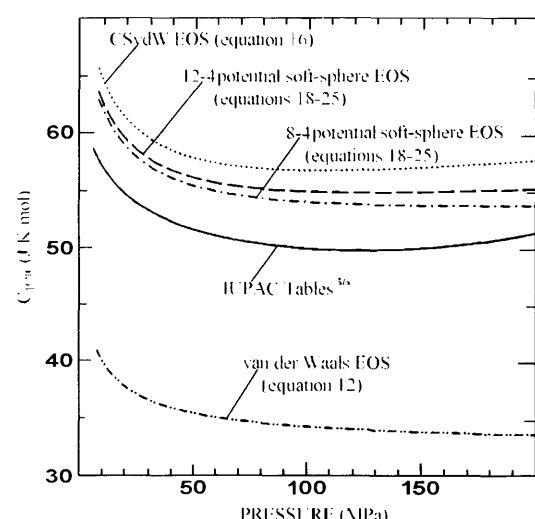


**Figure 9** Isobaric heat capacities  $C_p$  for liquid methane as a function of pressure at 140 K: comparison of experimental and derived  $C_p$  from various EOS.

## 8 Conclusions

The isobaric coefficient of thermal expansion, being the second derivative of the thermodynamic potential, is the most sensitive test for verification of equations of state. It can be measured by pressure-controlled scanning calorimetry over large ranges of pressure and temperature. The analysis of selected EOS of the van der Waals type has demonstrated the following:

the van der Waals EOS, and the EOS with the modified attractive term, do not correctly reproduce  $a_p(p, T)$  for simple liquids, nor correctly give the crossing point of its isotherms;

EOS of the van der Waals type with the repulsive part softer than the simple rigid-sphere term  $RT/(V_m - b)$  reproduce the crossing point of  $a_p(p, T)$  isotherms, although the absolute values are rather far from the calorimetric data;

the best reproduction of the isotherm crossing point is obtained when the rigid-sphere term in the van der Waals EOS is replaced by a soft-sphere repulsive term based on the 8–4 Lennard–Jones potential.

The above observations are similar for both *n*-hexane and methane as test substances, indicating that the anisotropy in the shape of interacting molecules has a minor effect on the high-density properties of simple liquids. The observations concerning the shape of the repulsive branch of the interacting pair potential are similar to the conclusions made on the basis of atomic scattering and shock compressions.<sup>18</sup> However, the information from the calorimetric method is much easier to derive from the EOS under investigation and to correlate with the intermolecular potential.<sup>2,3,21</sup> The observation that the crossing point of isotherms may be reproduced only with soft interacting pair potentials is to some extent similar to an attempt by the present author to explain the existence of the crossing point of  $a_p$  isotherms for simple dense liquids by the pressure-sensitive shape of the effective intermolecular potential.<sup>3</sup> For associated and self-associated liquids the situation is much more complicated, but as shown in the present article for *n*-hexanol and its binary mixtures with *n*-hexane for example, calorimetric information can serve as a guide in searching further for better EOS, which should include various specific interactions. It is also possible to extend this method to more complicated examples of condensed matter, as was demonstrated taking polyethylene as an example.

**Acknowledgements.** The content of the present article was partly presented at the 6<sup>th</sup> Polish Conference on Calorimetry and Thermal Analysis, Zakopane, September 1994, in a session presided over by Professor Mike Blandamer; the author is sincerely grateful for his kind invitation to publish that lecture in this issue of *Chemical Society Reviews*.

Financial support from the Polish Committee on Scientific Research under grant 7.S204.010.05 is gratefully acknowledged.

## 8 References

- 1 S. L. Randzio, *Pure Appl. Chem.*, 1991, **63**, 1409.
- 2 E. A. Moelwyn-Hughes, 'Physical Chemistry', Pergamon Press, Oxford 1961, pp. 321–342.
- 3 S. L. Randzio, *Phys. Lett. A*, 1986, **117**, 473.
- 4 P. W. Bridgman, *Proc. Am. Acad. Arts. Sci.*, 1913, **4**, 3.
- 5 S. L. Randzio, Calorimetric Determination of Pressure Effects, in 'Experimental Thermodynamics, Vol. IV: Solution Calorimetry', ed. K. N. Marsh and P. A. G. O'Hare, Blackwell, London 1994, pp. 303–324.
- 6 R. Fürth, *Proc. Cambridge Philos. Soc.*, 1941, **37**, 252.
- 7 V. P. Skripov, 'Metastable Liquids', Wiley, New York, 1974.
- 8 Ch. Alba, L. Ter Minassian, A. Denis, and A. Soulard, *J. Chem. Phys.*, 1985, **82**, 384.
- 9 L. Ter Minassian, K. Bouzar, and Ch. Alba, *J. Chem. Phys.*, 1988, **92**, 487.
- 10 V. G. Baonza, M. Cáceres, and J. Núñez Delgado, *J. Chem. Phys.*, 1993, **97**, 10813.
- 11 V. G. Baonza, M. Cáceres, and J. Núñez Delgado, *J. Chem. Phys.*, 1994, **98**, 1993.
- 12 V. G. Baonza, M. Cáceres, and J. Núñez, *Chem. Phys. Lett.*, 1993, **216**, 579.
- 13 J. D. van der Waals, Doctoral Dissertation, Leiden, 1873.
- 14 T. W. Leland, Jr. and P. S. Chappelar, *Ind. Eng. Chem.*, 1968, **60**, 15.
- 15 H. C. Longuet-Higgins and B. Widom, *Mol. Phys.*, 1964, **8**, 549.
- 16 G. A. Monsori, N. F. Carnahan, K. E. Starling, and T. W. Leland, *J. Chem. Phys.*, 1971, **54**, 1523.
- 17 J. D. Weeks, D. Chandler, and H. C. Andersen, *J. Chem. Phys.*, 1971, **54**, 5237.
- 18 K. S. Pitzer and S. M. Sterner, *J. Chem. Phys.*, 1994, **101**, 3111.
- 19 S. L. Randzio and U. K. Deiters, Thermodynamic testing of equations of state of dense simple liquids, *Ber. Bunsenges. Phys. Chem.*, 1995, **99**, in press.
- 20 U. K. Deiters, *Mol. Phys.*, 1991, **74**, 153.
- 21 U. K. Deiters and S. L. Randzio, *Fluid Phase Equil.*, 1995, **103**, 199.
- 22 S. L. Randzio, *Thermochimica Acta*, 1985, **89**, 215.
- 23 S. L. Randzio, J.-P. E. Grolier, and J. R. Quint, *Rev. Sci. Instrum.*, 1994, **65**, 960.
- 24 S. L. Randzio, D. J. Eatough, E. A. Lewis, and L. D. Hansen, *J. Chem. Thermodyn.*, 1988, **20**, 937.
- 25 L. Ter Minassian and Ph. Pruzan, *J. Chem. Thermodyn.*, 1977, **9**, 375.
- 26 Tables of standard reference data for *n*-hexane. 'Thermodynamic Properties in the Ranges 180–630 K and 0.1–100 MPa', GSSSD 90–85 (USSR State Committee on Standards, Moscow, 1986) (in Russian).
- 27 Ph. Pruzan, *J. Phys. Lett. (Paris)*, 1984, **45**, L273.
- 28 Ph. Pruzan, *J. Chem. Thermodyn.*, 1991, **23**, 247.
- 29 S. L. Randzio, J.-P. E. Grolier, J. R. Quint, D. J. Eatough, E. A. Lewis, and L. D. Hansen, *Int. J. Thermophys.*, 1994, **15**, 415.
- 30 R. D. Goodwin, *J. Phys. Chem. Ref. Data*, 1988, **17**, 1541.
- 31 A. H. Fuchs, Ph. Pruzan, and L. Ter Minassian, *J. Phys. Chem. Solids*, 1979, **40**, 369.
- 32 B. W. Street, *Physica*, 1974, **76**, 59.
- 33 O. Redlich and J. N. S. Kwong, *Chem. Rev.*, 1949, **44**, 233.
- 34 G. Soave, *Chem. Eng. Sci.*, 1972, **27**, 1197.
- 35 D.-Y. Peng and D. B. Robinson, *Ind. Eng. Chem. Fundam.*, 1976, **15**, 59.
- 36 S. Angus, B. Armstrong, and K. M. de Reuck, 'International Thermodynamic Tables of the Fluid State, Vol. V, Methane', Pergamon Press 1978.
- 37 N. F. Carnahan and K. E. Starling, *J. Chem. Phys.*, 1969, **51**, 635.
- 38 N. F. Carnahan and K. E. Starling, *AIChE J.*, 1972, **18**, 1184.
- 39 S. L. Randzio, E. A. Lewis, D. J. Eatough, and L. D. Hansen, *Int. J. Thermophys.*, 1995, **16**, 883.
- 40 L. Ter Minassian, Ph. Pruzan, and A. Soulard, *J. Chem. Phys.*, 1981, **75**, 3064.
- 41 S. L. Randzio, J.-P. E. Grolier, and J. R. Quint, *J. Therm. Anal.*, 1992, **38**, 1960.
- 42 U. K. Deiters, *Fluid Phase Equil.*, 1993, **89**, 229.
- 43 D. J. Pastine, *J. Chem. Phys.*, 1968, **49**, 3012.
- 44 D. J. Pastine, *J. Appl. Phys.*, 1970, **41**, 5085.
- 45 L. Rodier-Renaud, S. L. Randzio, J.-P. E. Grolier, J. R. Quint, and J. Jarrin, Isobaric thermal expansivities of polyethylenes with various crystallinities over the pressure range from 0.1 MPa to 300 MPa and over the temperature range from 303 K to 393 K, *J. Polym. Sci., Polym. Phys. Ed.* (submitted).
- 46 E. H. Brown, *Bull. Inst. Int. Froid. Annexe*, 1960–61, 169.
- 47 J. S. Rowlinson, *Rep. Progr. Phys.*, 1965, **28**, 169.